Published online 24 June 2009

Nucleic Acids Research, 2009, Vol. 37, No. 17 ***e114***
doi:10.1093/nar/gkp540

Preparation of selective and segmentally labeled single-stranded DNA for NMR by self-primed PCR and asymmetrical endonuclease double digestion

Frank H. T. Nelissen, Frederic C. Girard, Marco Tessari, Hans A. Heus and Sybren S. Wijmenga*

Department of Biophysical Chemistry, Institute for Molecules and Materials, Radboud University Nijmegen, Toernooiveld 1, 6525 ED Nijmegen, the Netherlands

Received April 7, 2009; Revised and Accepted June 9, 2009

ABSTRACT

We demonstrate a new, efficient and easy-to-use method for enzymatic synthesis of (stereo-)specific and segmental $^{13}C/^{15}N/^{2}H$ isotope-labeled single-stranded DNA in amounts sufficient for NMR, based on the highly efficient self-primed PCR. To achieve this, new approaches are introduced and combined. (i) Asymmetric endonuclease double digestion of tandem-repeated PCR product. (ii) T4 DNA ligase mediated ligation of two ssDNA segments. (iii) *In vitro* dNTP synthesis, consisting of *in vitro* rNTP synthesis followed by enzymatic stereo-selective reduction of the C2′ of the rNTP, and a one-pot add-up synthesis of dTTP from dUTP. The method is demonstrated on two ssDNAs: (i) a 36-nt three-way junction, selectively $^{13}C_9/^{15}N_3/^{2}H_{(1',2'',3',4',5',5'')}$-dC labeled and (ii) a 39-nt triple-repeat three-way junction, selectively $^{13}C_9/^{15}N_3/^{2}H_{(1',2'',3',4',5',5'')}$-dC and $^{13}C_9/^{15}N_2/^{2}H_{(1',2'',3',4',5',5'')}$-dT labeled in segment C20-C39. Their NMR spectra show the spectral simplification, while the stereo-selective ^{2}H-labeling in the deoxyribose of the dC-residues, straightforwardly provided assignment of their C1′–H2′ and C2′–H2′ resonances. The labeling protocols can be extended to larger ssDNA molecules and to more than two segments.

INTRODUCTION

Isotope labeling has contributed markedly to the success of multi-dimensional hetero-nuclear NMR spectroscopy in structure and dynamics investigations of proteins (1–5), RNAs (6–28), DNAs (28–37), and their complexes (38–41). For proteins and RNAs, isotope labeling has become standard practice. In sharp contrast, for (larger) ds/ssDNAs application of isotope-labeling still lags far behind, largely due to a lack of comparably simple, flexible and cost-efficient methods for their synthesis.

Labeling of DNA by chemical synthesis is versatile and been used to produce ds/ssDNAs, labeled uniformly (29,36) or selectively/site-specifically (32,34,37,42–44) with $^{13}C/^{15}N$ isotopes or segmentally (30,31) with $^{13}C/^{2}H$ isotopes, using tailor-made phosphoramidites. However, their synthesis requires specialized chemical expertise, is labor intensive and costly. Enzymatic synthesis has therefore been more popular in the field of DNA structural biology, and *in vivo* (45,46) and *in vitro* (45,47–57) methods have been developed.

In the *in vivo* methods plasmids are amplified in *E. coli* cells grown on labeled minimal medium (45,46). The plasmids contain multiple repeats of the desired sequence with each repeat flanked by an endonuclease-sensitive site. After enzymatic digestion single double-stranded (ds) DNA fragments are released. Although this method circumvents the requirement of isotope-labeled dNTPs, it restricts the types of labeling (see below) and is relatively inefficient.

Enzymatic *in vitro* synthesis of isotope-labeled ssDNA was first achieved by Zimmer and Crothers by means of a template-driven fill-in reaction (47). This method employs a DNA polymerase I fill-in reaction on the single-stranded region of a hairpin-primed DNA template, using isotope-labeled dNTPs as building blocks. A ribonucleoside is placed at the 3′-terminus of the hairpin, so that upon alkaline hydrolysis the synthesized isotope-labeled ssDNA is released. Modifications leading to improved efficiency have been reported (48,49), while Mer and Chazin (50)

*To whom correspondence should be addressed. Tel: +31 24 3652678; Fax: +31 24 3652112; Email: s.wijmenga@nmr.ru.nl

The authors wish it to be known that, in their opinion, the first two authors should be regarded as joint First Authors.

described a modification that allows for segmental isotope labeling. The template-driven fill-in reaction is relatively straightforward. A drawback is the need for stoichiometric amounts of expensive modified DNA template.

A second *in vitro* method is Endonuclease-Sensitive Repeat Amplification (ESRA) (45,55). It is based on a self-primed PCR amplification, originally called Concatemer Chain-Reaction (51,52), in which a dsDNA template of tandem repeats is elongated using (isotope-labeled) dNTPs by means of PCR in a number of cycles of heating, annealing and extension. This amplification produces long dsDNAs consisting of multimeric repeats of the target sequence. Endonuclease-sensitive sites flank the individual dsDNA repeats (45), so that restriction enzyme digestion releases the target dsDNA. Improvements have been reported in terms of sequence flexibility (56) and length of produced target dsDNA (57). It has also been proposed to attain PCR amplification of tandem repeats in a plasmid (53,54). However, this PCR protocol is more involved and most importantly, not self-primed and thus requires stoichiometric amounts of primer. The principal advantages of the self-primed PCR amplification are its simplicity and high efficiency. A single dsDNA template leads to copious amounts of isotope-labeled dsDNA targets, instead of one DNA target per template molecule as in the template-driven fill-in reaction. Drawbacks are that only dsDNA can be produced and that the existing protocol does not allow for segmental labeling.

Both *in vitro* methods need isotope-labeled dNTPs as building blocks. For RNA, isotope labeling—via *in vitro* synthesis—is common practice, because the required rNTP building blocks are readily available with a variety of labeling patterns; the rNTPs can either be uniformly labeled with $^{2}H/^{13}C/^{15}N$ isotopes (6,7,10,11,14), when extracted from bacterial cells, or (stereo-)selectively labeled with $^{2}H/^{13}C/^{15}N$ isotopes (9,12,13,15,17,27), when produced via *in vitro* synthesis. However, for dNTPs the situation is less favorable. The dNTP production methods involve extraction of isotope-labeled dNMPs from genomic (bacterial) DNA (14,47,48,58), which leads to limited yields as compared to rNTPs (RNA) and restricts the labeling to mainly uniformly in ^{13}C, ^{15}N, and/or ^{2}H. The *in vitro* synthesis of (stereo-) selectively $^{2}H/^{13}C/^{15}N$-labeled rNTPs is at present not available for dNTPs.

In conclusion, the ESRA stands out for its simplicity and efficiency among the existing methods for production of isotope-labeled DNA. However, ESRA has three main drawbacks: (i) only dsDNA can be produced, (ii) segmental labeling is not possible and (iii) existing production methods for the required dNTPs have limitations in terms of available amounts and variety in labeling pattern.

In this contribution, we present a new, efficient and easy-to-use method for the large-scale *in vitro* synthesis of isotope-labeled DNA. It is based on ESRA and we introduce new approaches to resolve the above-mentioned drawbacks. Synthesis of ssDNA, instead of only dsDNA, is now possible by introducing asymmetrical digestion of PCR products. The labeling can either be overall or segmental. In the residues, the labeling can be uniform, or (stereo-)selective with $^{2}H/^{13}C/^{15}N$ isotopes, depending on the dNTPs employed. Our method includes a protocol for the efficient synthesis of dNTPs obtained by reduction of *in vitro* synthesized rNTPs, thereby connecting the versatility of RNA labeling to DNA. The method is demonstrated via the synthesis and NMR of a 36-nt three-way junction ssDNA (59) and a 39-nt triple-repeat three-way junction ssDNA (60,61).

MATERIALS AND METHODS

Folding simulations of PCR primers and DNA segments for the (segmental) labeling of ssDNA

Predictions of the thermodynamic stability of intramolecular folds, self-complementary duplexes and the (desired) hybrids of the used DNA sequences were obtained using DINAMelt (62). In the DINAMelt simulations for the PCR sequences, the DNA concentration was 0.1 μM and salt concentrations 10 mM NaCl and 2 mM Mg^{2+}, comparable to the conditions during PCR amplifications. In the DINAMelt simulations for the ligation, the DNA concentration was 10 μM and the NaCl and Mg^{2+}-concentrations were each 10 mM, matching the conditions during DNA ligation.

Synthesis of $^{13}C_9/^{15}N_3/^{2}H_{(1',2'',3',4',5',5'')}$-dCTP and $^{13}C_9/^{15}N_2/^{2}H_{(1',2'',3',4',5',5'')}$-dTTP

For calculation of yields, here and below, all concentrations of purified intermediate and final products were determined by UV absorption unless otherwise stated. Prior to dTTP and dCTP synthesis, UTP residues were *in vitro* synthesized from 450 μmol $^{13}C_6/^{2}H_7$-D-glucose and 440 μmol $^{13}C_4/^{15}N_2$-uracil (Cambridge Isotope Laboratories, Andover, MA, USA) using enzymes of the glycolysis and pentose phosphate pathway (9,12,13,63) (see Supplementary Data for a detailed description). $^{13}C_9/^{15}N_3/^{2}H_{(1',3',4',5',5'')}$-CTP residues were synthesized in a 120 ml reaction mixture containing 0.5 mM (60 μmol) $^{13}C_9/^{15}N_2/^{2}H_{(1',3',4',5',5'')}$-UTP, 10 mM $^{15}NH_4Cl$ and 7.5 units CTP synthase (64) (Supplementary Data). The UTP and CTP were separated from their ATP cofactor on an Akta Basic equipped with a HiLoad Q Sepharose HP column (GE Healthcare) using a linear gradient from 50–350 mM NaCl in Milli-Q water (Millipore) at pH 9. Nucleotide containing fractions were desalted on a Sephadex G10 column (ø2.5 × 30 cm), lyophilized and dissolved to 100 mM in Milli-Q water.

Fifty-nine micromoles CTP and 60 μmol UTP were exchanged with D_2O by lyophilization for three times in 1 ml D_2O. A 5× concentrate of reduction buffer (20 mM HEPES (pH 7.5), 30 mM DTT, 0.5 mM EDTA and 1 M NaAc) was exchanged with D_2O by vacuum concentration to dryness for three times in D_2O, subsequently dissolved in D_2O and the pD adjusted to 7.5 with 10 M NaOD. D_2O exchanged CTP and UTP were added to a final concentration of 1 mM in separate reactions and 5 μl of 20 mg/ml ribonucleotide triphosphate reductase (RTPR) (65,66) (Supplementary Data) along with 10 μl of 5 mM coenzyme B12 in D_2O were added per ml of reduction buffer and incubated for 1 h at 37°C in the dark. The reduction

progress was checked by reversed phase chromatography (RPC) on a PepRPC 15 HR10/10 column (GE Healthcare) by applying a 20 ml linear gradient from 50 mM TEAA (pH 7) to 40% 50 mM TEAA (pH 7) + 30% acetonitril. The reaction mixtures were purified over a Dowex 1x2 anion exchange column (Sigma-Aldrich, Zwijndrecht, The Netherlands) using a linear gradient from 0 to 1 M NaCl. Nucleotide containing fractions were desalted and concentrated to 5 mM in Milli-Q water and stored at −20°C.

dTTP was synthesized in a one-pot add-up reaction from dUTP. All reactions were checked by RPC applying a 20 ml linear gradient from 0.2 M KH_2PO_4 (pH 4) to 40% 0.2 M K_2HPO_4 (pH 4) + 30% methanol. Twenty milliliter of 1.3 mM dUTP in 20 mM Tris–HCl (pH 8.1 at 25°C) + 5 mM $MgCl_2$ was incubated at 85°C for 1 h in the presence of 125 ng/ml His_6-tagged *Pfu* dUTPase (67) (Supplementary Data). The reaction mixture was adjusted to 0.25 mM dUMP in 40 mM Tris–HCl (pH 7.5), 50 mM $MgCl_2$, 100 mM β-mercaptoethanol, 2.3 mM formaldehyde and 2 mM (6R,S)-5,10-methylene-5,6,7,8-tetrahydrofolic acid (Schircks Laboratories, Switzerland). His_6-tagged *E. coli* thymidylate synthase (68) (Supplementary Data) was added to 50 μg/ml and incubated overnight at 37°C. The reaction mixture was again adjusted by adding KCl to 80 mM, phosphoenolpyruvate to 10 mM, ATP to 0.05 mM, pyruvate kinase (Sigma) to 2.5 U/ml and his_6-tagged bacteriophage T5 dNMP kinase (69) (Supplementary Data) to 100 μg/ml and then incubated at 37°C for another 3 h.

Synthesis of $^{13}C_9/^{15}N_3/^{2}H_{(1',2'',3',4',5',5'')}$-dC selective labeled three-way junction ssDNA by self-primed PCR (Figure 1 and Table 1)

All restriction endonucleases and buffers were purchased from Fermentas. In step 1, 10 PCR reactions of 400 μl were carried out in PCR buffer with 2 mM $MgSO_4$ containing 0.2 mM of each dGTP, dATP, dTTP, $^{13}C_9/^{15}N_3/^{2}H_{(1',2'',3',4',5',5'')}$-dCTP, 0.1 μM of primers 3W-sense and 3W-asense (Table 1). Each PCR mixture contained 80 ng of His_6-tagged *Pfu* DNA polymerase (70) (Supplementary Data) and 10 ng of His_6-tagged *Pfu* dUTPase. Mixtures were cycled 30 times in a Progene thermal cycler (Techne) at 95°C for 90 s, at 65°C for 90 s and at 72°C for 6 min and 30 s and followed by a final filling step at 72°C for 20 min. In step 2, 80 PCRs of 400 μl were carried out under the same conditions as in step 1 PCRs, except a 10 times dilution of step 1 PCR product served as DNA template instead of the primers 3W-sense and 3W-asense. The PCR mixtures were pooled, diluted to 200 ml buffer R^+ and digested for 3 h at 37°C with 2.5 kU of 5′-**CGCG**-3′ cleaving *Bsh*1236I. The digestion mixture was purified over a ResourceQ 6 ml column (GE Healthcare) using a linear gradient from 0 to 1.5 M NaCl in 10 mM sodium phosphate buffer (pH 7.4), desalted by ethanol precipitation and dissolved in 120 ml buffer *Eco*RI. Total 10 kU of *Eco*RI (5′-**GAATTC**-3′) was added and incubated at 37°C for 3 h. The digested DNA was purified over a ResourceQ column, desalted in an YM-3 centricon (Millipore) and subsequently, electrophorized on a preparative 20% denaturing polyacrylamide gel (PAGE) containing 8 M urea. The band of 36-nt three-way junction ssDNA was electroeluted from the gel in an Elutrap device (Schleicher & Schuell) and subsequently washed with 20 mM sodium phosphate buffer (pH 7.5) containing 1 M NaCl + 50 mM EDTA and Milli-Q water. Finally, the DNA was exchanged two times with 1 ml D_2O by lyophilization.

Synthesis of $^{13}C_9/^{15}N_2/^{2}H_{(1',2'',3',4',5',5'')}$-dT and $^{13}C_9/^{15}N_3/^{2}H_{(1',2'',3',4',5',5'')}$-dC selective and segmental labeled triple-repeat junction 6 wt ssDNA

The 20 nt ssDNA segment junction 6 wt-p2 (C20-C39; Table 1) for ligation was obtained by self-primed PCR (Figure 1) as for the three-way junction ssDNA with the case specific modifications as described hereafter. The unlabeled dTTP in the PCR mixtures was substituted by $^{13}C_9/^{15}N_2/^{2}H_{(1',2'',3',4',5',5'')}$-dTTP and the amplification primers were junction 6 wt-p2-sense and junction 6 wt-p2-asense (Table 1). Blunt end digestion of the amplified DNA was carried out with 2.5 kU of *Pvu*II (5′-**CAGCTG**-3′) in buffer G^+ and the second digestion with 10 kU *Xho*I (5′-**CTCGAG**-3′) in buffer R^+.

The purified 20-nt junction 6 wt-p2 ssDNA segment was ligated to the 19-nt junction 6 wt-p1 ssDNA segment (Table 1) in an 11 ml preparative ligation reaction containing 7.5 μM of junction 6 wt-p2, 10 μM of junction 6 wt-p1 and 10 μM of the 28-nt DNA splint (Table 1) in T4 DNA ligase buffer. The reaction was heated 2 min at 95°C and incubated 10 min at room temperature prior to the addition of 2.8 kU T4 DNA ligase and followed by ligation at 37°C for 4 h. The 39-nt ligation product was purified from denaturing PAGE as described before and lyophilized.

NMR experiments

The three-way junction ssDNA sample was dissolved in 50 mM NaCl in D_2O (pD 5.6), to 0.2 mM and the full junction 6 wt ssDNA was dissolved in 10 mM sodium phosphate pH 6.7 containing 0.1 mM EDTA and 7% D_2O to 0.2 mM. The samples were heated at 95°C, snap-cooled on ice-water and transferred to a Shigemi NMR tube. All NMR spectra were acquired at 25°C using a Varian 600 Inova spectrometer equipped with a shielded triple-axis gradient HCN probe. A 2D H2′C2′C1′ experiment was recorded for the stereo-specific assignment of the H2′ of the cytidines by observation of (C1′, H2′) correlations via the relayed H2′→C2′→C1′ connectivity's. The 2D spectrum was acquired with 128 scans per increment as a data matrix of $160(t_1) \times 614(t_2)$ complex points, with sweep widths of 9000 (^{13}C) and 8000 Hz (^{1}H). A 1D imino spectrum of junction 6 wt was acquired with 256 scans, a recovery delay of 2 s and an acquisition time of 80 ms. Selective water-flip-back pulses were employed to prevent saturation of the water resonance and attenuation of the imino protons signals. A (^{15}N, ^{1}H) HSQC pulse scheme was used to acquire a 1D ^{15}N-edited spectrum of imino protons from ^{15}N-labeled thymidine nucleotides. A 2D (^{15}N, ^{1}H) HSQC was recorded with 64 scans per increment as a data matrix of $80(t_1) \times 1120(t_2)$

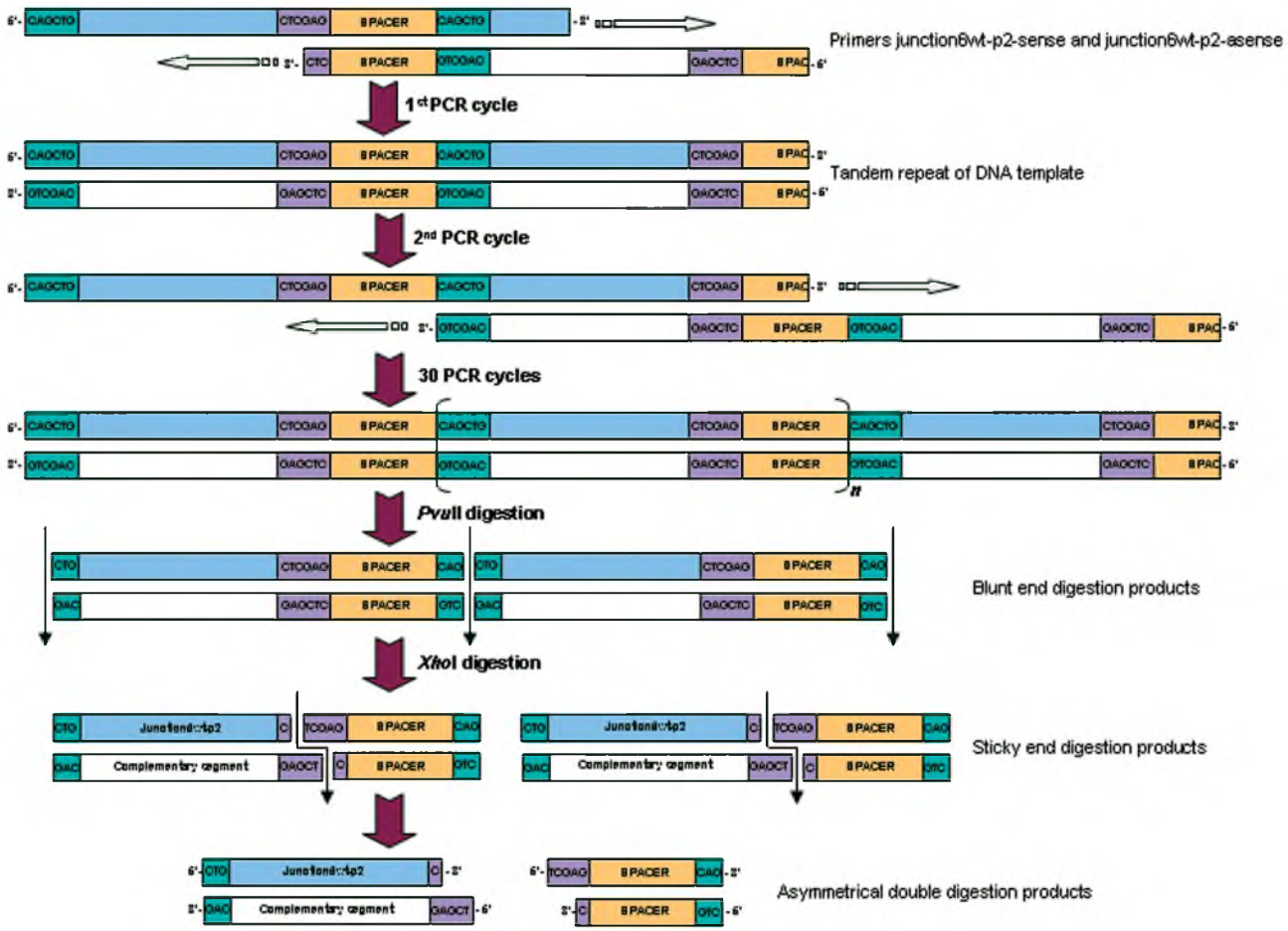

Figure 1. Schematic of the proposed primer-pair amplification by self-primed PCR, here shown for the 20-nt junction 6 wt-p2 ssDNA sequence (see below). The two designed primers hybridize to form an amplifiable overlap that is filled-in by *Pfu* DNA polymerase in the first PCR cycle. The formed tandem repeat of dsDNA will be elongated in the next stages of cycling by the possibility to shift annealing position of the tandem repeated dsDNA. After 30 cycles, the long DNA is digested with a blunt-end-generating endonuclease followed by digestion with a sticky-end-generating endonuclease. The asymmetry in the digested DNA molecules allows for separation of the four individual strands on denaturing PAGE.

complex points, with sweep widths of 1000 Hz (^{15}N) and 16 000 Hz (^{1}H).

RESULTS

We describe and demonstrate an efficient and easy-to-use self-primed PCR method for the enzymatic synthesis of isotope-labeled dsDNA and/or ssDNA, for which we introduce and combine three new approaches.

(i) *Self-primed PCR followed by asymmetric endonuclease double digestion to produce ssDNA (Figure 1)*. This method originates from the highly efficient and straightforward self-primed PCR-based ESRA technique described by Louis *et al.* (45) for the synthesis of isotope-labeled dsDNA. As in ESRA, long tandem-repeated dsDNA PCR products are synthesized by self-primed PCR in a number of heating/annealing cycles using *Pfu* DNA polymerase. The major modification we introduce lies in the enzymatic digestion of the PCR products, which allows for separation of the PCR products into ssDNAs. Instead of using a single blunt-end digestion, we generate asymmetrical dsDNA in two successive digestions. The double-digested products migrate distinguishably on denaturing PAGE. The desired ssDNA fragment can be used for NMR structural analysis directly after purification from gel.

(ii) *Segmental labeling via DNA-splinted ligation (Table 1)*. Segmental labeled ssDNA can efficiently be produced by T4 DNA ligase mediated ligation of a labeled to unlabeled strand of DNA assisted by a complementary DNA splint.

(iii) *In vitro synthesis of isotope-labeled dNTPs (Figure 2)*. *In vitro* production of rNTPs allows for a large variety of labeling patterns including deuteration (9,12,13,63). We demonstrate that (stereo-)selective or uniformly ^{2}H/^{13}C/^{15}N-labeled dNTPs are efficiently obtained by *in vitro* rNTP synthesis (9,12,13,63) followed by enzymatic reduction of the C2′ hydroxyl of the produced rNTPs (65,66).

The whole method is demonstrated on the synthesis of a 36-nt three-way junction ssDNA (59) (Figure 2C, left)

Table 1. Overview of used and synthesized ssDNA sequences

Sequence name	Nucleotide sequence	Utilization
3W-sense	5′**CGCGT**GCAGCGGCTTGCCGGCACTTGTGCTTCTGCAC**GAATTC**CAACCGG**CGCGT**GCAGCGGCTT-3′	PCR
3W-asense	5′CCGGTTG**GAATTC**GTGCAGAAGCACAAGTGCCGGCAAGCCGCTGCA**CGCG**CCGGTTG-3′	PCR
Junction 6 wt-p2-sense	5′**CAGCTG**CCCTTGGGCTGCTCCGC**TCGAG**ACGTCGC***CAGCTG*****CCCTTGG***-3′	PCR
Junction 6 wt-p2-asense	5′GCGACGT**CTCGAG**CGGAGCAGCCCAAGGG**CAGCTG**GCGACGT**CTC**-3′	PCR
Junction 6 wt-p1	5′GCGGAGCAGCACCTTGGTG-3′	Ligation
Junction 6 wt-p2	5′**CTG**CCCTTGGGCTG**C**TCCGC-3′	Ligation
DNA splint	5′CAGCCCAAGGGCA*G*CACCAAGGTGCTGC-3′	Ligation
Three-way junction	5′**CG**TGCAGCGGCTTGCCGGCACTTGTGCTTCTGCAC**G**-3′	NMR
Junction 6 wt	5′GCGGAGCAGCACCTTGGTG**CTG**CCCTTGGGCTGCTCCG**C**-3′	NMR

Sequence names shown in bold represent synthesized labeled sequences; all others are unlabeled and obtained from Biolegio (Nijmegen, the Netherlands). Nucleotides of PCR primers shown in italics represent (a part of) the desired ssDNA sequence to be obtained. Nucleotides depicted in bold represent (a part of) endonuclease sites and underlined parts represent the desired overlap to be formed during PCR and/or ligation.

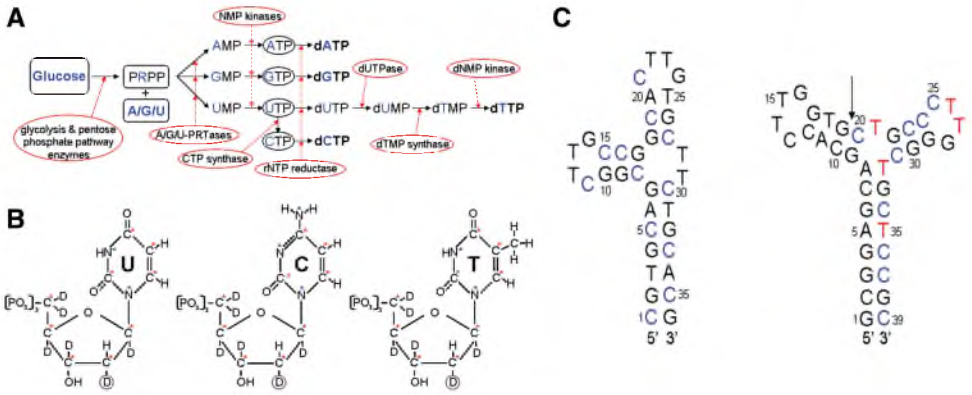

Figure 2. (**A**) *In vitro* (deoxy)ribonucleotide triphosphate synthesis. Labeled starting materials are shown in bold and blue. Labeled rNTPs, here as intermediate products, are circled. Labeled end-product dNTPs are shown in bold. The enzymes catalyzing different reactions are circled. See text for detailed description of the reactions. (**B**) Overview of the *in vitro* synthesized labeled dNTPs. From left to right: $^{13}C_9/^{15}N_2/^{2}H_{(1',2'',3',4',5',5'')}$-dUTP, $^{13}C_9/^{15}N_3/^{2}H_{(1',2'',3',4',5',5'')}$-dCTP and $^{13}C_9/^{15}N_2/^{2}H_{(1',2'',3',4',5',5'')}$-dTTP. The red asterisks at carbon atoms indicate ^{13}C labels; the blue asterisks at nitrogen atoms indicate ^{15}N labels. The circled deuteron indicates the introduced stereo-selective deuteration in the sugar moiety during rNTP reduction. (**C**) Predicted most stable secondary structures of the three-way junction ssDNA (left) and the triple-repeat three-way junction ssDNA (junction 6 wt, right). The arrow indicates the chosen segmentation site in junction 6 wt. Blue cytidine residues are $^{13}C_9/^{15}N_3/^{2}H_{(1',2'',3',4',5',5'')}$-labeled (see also **B**) and red thymidine residues are $^{13}C_9/^{15}N_2/^{2}H_{(1',2'',3',4',5',5'')}$. (see **B**).

(stereo-)selectively labeled on the cytidine residues and a 39-nt triple-repeat three-way junction ssDNA (60,61) (Figure 2C, right) that is (stereo-)selectively labeled on the cytidine and thymidine residues of segment C20–C39.

Design of PCR amplification primers and segments

The PCR primer pairs are designed to contain both target sequence and endonuclease digestion sites (Figure 1 and Table 1). It is essential that during PCR amplification the desired hybridization of primers indeed occurs and alternative stable structures do not interfere. Table 2 provides an overview of the predicted folds and stabilities of the PCR primers and their hybridization products as predicted by DINAMelt ('Materials and Methods' section). For all four individual primers, neither unfavorable intramolecular folds nor unfavorable self-complementary duplexes are predicted. Although, a non-amplifiable hybrid is predicted to be more stable than the desired amplifiable hybrid (ΔG values inside versus outside parentheses, Table 2), it is expected (and ultimately experimentally proven) not to block PCR, because both hybrids will occur in the annealed mixture.

For the segmental labeling of the junction 6 wt ssDNA (Figure 2C, right), the molecule was divided into junction 6 wt-p1 (19-nt, residue 1–19) and junction 6 wt-p2 (20 nt; residue 20–29), so that the latter encompasses the two thymidine residues present in the structurally interesting junction region. DINAMelt simulations were performed to assess the potential presence of alternative secondary structures that could interfere with ligation (Table 2). The desired hybridization with the DNA splint was predicted to be most stable.

Synthesis of $^{13}C_9/^{15}N_3/^{2}H_{(1',2'',3',4',5',5'')}$-dCTP and $^{13}C_9/^{15}N_2/^{2}H_{(1',2'',3',4',5',5'')}$-dTTP

The *in vitro* synthesis of $^{13}C_9/^{15}N_2/^{2}H_{(1',2'',3',4',5',5'')}$-UTP yielded 390 µmol of UTP out of 450 µmol $^{13}C_6/^{2}H_7$-D-glucose and 440 µmol $^{13}C_4/^{15}N_2$-uracil, a yield of 89%.

The subsequent synthesis of $^{13}C_9/^{15}N_3/^{2}H_{(1',2'',3',4',5',5'')}$-CTP, out of 60 µmol UTP, yielded 59 µmol of CTP. The reduction of 60 µmol UTP and 59 µmol CTP by RTPR led to 58 µmol dUTP and 56 µmol of dCTP, yields of 96.5% and 95%. The dephosphorylation of dUTP proceeded for over 99%, the subsequent methylation of dUMP to dTMP for 93%, and the phosphorylation to dTTP for 98%, yielding 52 µmol of dTTP. The overall yields for the synthesis of dTTP and dCTP from glucose and uracil were 77% and 83%.

Table 2. Predicted hybridization and folding stabilities of ssDNA sequences

DNA strand(s)	Intramolecular (ΔG)	Duplex (ΔG)	Hybrid (ΔG)
3W-sense	−11.7	−18.5	NA
3W-asense	−7.2	−17.6	NA
3W-sense + 3W-asense	NA	NA	−30.8* (−67.4)
Junction 6 wt-p2-sense	−5.8	−13.8	NA
Junction 6 wt-p2-asense	−6.3	−17.4	NA
Junction 6 wt-p2-sense + Junction 6 wt-p2-asense	NA	NA	−29.1* (−47.9)
Junction 6 wt-p1	−3.0	−6.0	NA
Junction 6 wt-p2	−3.1	−9.1	NA
DNA splint	−7.4	−19.3	NA
DNA splint + junction 6 wt-p1	NA	NA	−18.0
DNA splint + junction 6 wt-p2	NA	NA	−17.8
DNA splint + junction 6 wt	NA	NA	−39.1

ΔG values are in kcal/mol at 37°C. Simulation conditions are 10 mM NaCl, 2 mM Mg^{2+} and 0.1 µM strand concentration for simulations with PCR primers and 10 mM NaCl, 10 mM Mg^{2+} and 10 µM strand concentration for simulations concerning ligation. ΔG values with an asterisk represent the stability of the desired hybridization between the parts of the PCR primer pairs, whereas the ΔG value in parentheses represents the stability of a non-amplifiable hybrid between the primer pairs.

Synthesis of selective and/or segmentally labeled ssDNA

In step 1 of the self-primed PCR protocol (Materials and Methods section and Figure 1), PCRs with the primer pairs 3W-sense + 3W-asense and junction 6 wt-p2-sense + junction 6 wt-p2-asense, yielded primarily high molecular weight DNA (>>10 kb; the main band is located near the loading slot in Figure 3A and B, lanes 1). The step 1 PCR-product of the junction 6 wt DNA (Figure 3B, lane 1) was substantially more smeared out than the step 1 PCR-product of the three-way junction DNA (Figure 3A, lane 1). The subsequent PCRs in step 2 yielded for both constructs even more high molecular weight DNAs, as evident from the reduced smearing (Figure 3A and B, lanes 1 and 2); note again that the main band of PCR products is located near the loading slot, indicating high molecular weight DNAs (Figure 3A and B, lanes 2).

This main band disappeared completely after blunt-end-generating endonuclease digestion and single bands below the 100 bp marker were observed (Figure 3A and B, lanes 3). The latter could be attributed to the expected 50 bp (3.75 mg; 0.12 µmol) and 35 bp (2.5 mg; 0.11 µmol) digestion products for the three-way junction and junction

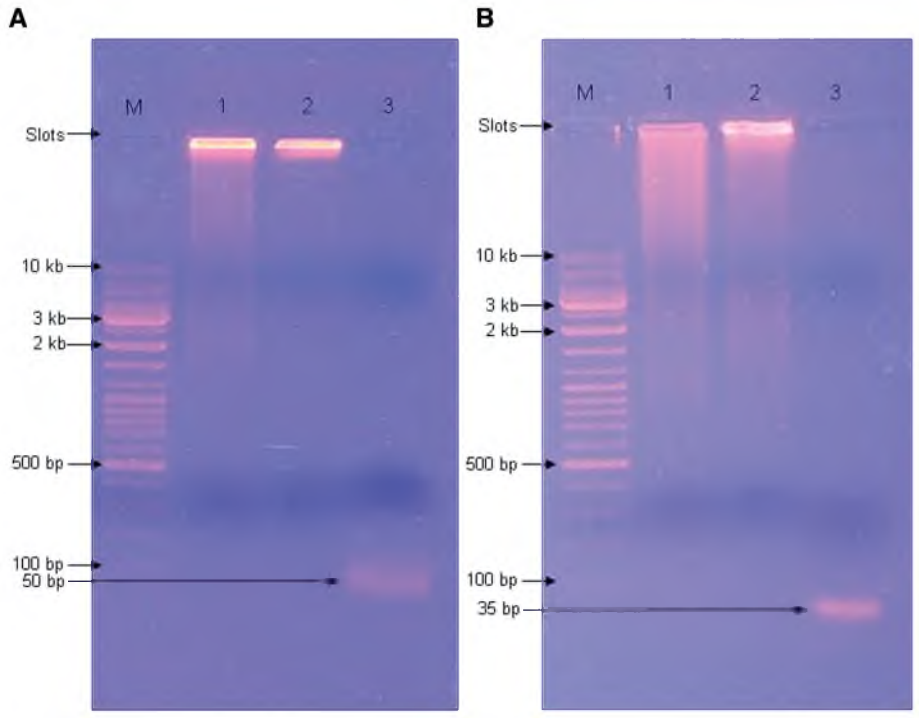

Figure 3. Progress of the PCR amplifications of three-way junction DNA and junction 6 wt DNA on 0.8% agarose. (**A**) Lanes 1–3 contain the following samples: (1) 10 µl of step 1 PCR mix of three-way junction DNA, (2) 10 µl of step 2 PCR mix, (3) 10 µl *Bsh*1236I digestion mixture. (**B**) Lanes 1–3 contain the following samples: (1) 10 µl of step 1 PCR mix of junction 6 wt DNA, (2) 10 µl of step 2 PCR mix, (3) 10 µl *Pvu*II digestion mixture. Lanes M contain 5 µl of gene-ruler DNA Ladder Mix (Fermentas). Bands are visualized with ethidiumbromide (Sigma-Aldrich, Zwijndrecht, The Netherlands).

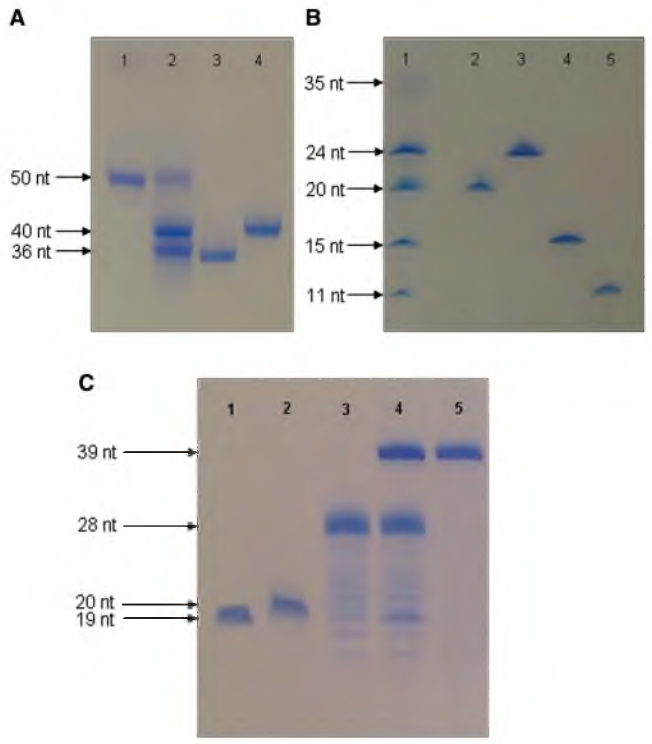

Figure 4. Digestion products generated after successive endonuclease digestion of blunt dsDNA fragments. (**A**) Lanes 1–4 contain the following samples: (1) 1 µg of the 50 bp *Bsh*1236I digest of the long repeated DNA, (2) 2.5 µg of *Eco*RI digested 50 bp three-way junction dsDNA. (3) 1 µg of 36-nt 3way-junction ssDNA (4) 1 µg of the complementary 40-nt sequence. (**B**) Lanes 1–5 contain the following samples: (1) 2 µg *Xho*I digested 35 bp junction 6 wt-p2 dsDNA, (2) 1 µg of purified junction 6 wt-p2 ssDNA, (3) 1 µg of the complementary 24-nt fragment, (4) 1 µg of 15 nt spacer fragment, (5) 1 µg 11-nt spacer fragment. (**C**) Course of the segmental labeling of junction 6 wt ssDNA. Lanes 1–5 contain the following samples: (1) 1.25 µg of junction 6 wt-p1 ssDNA, (2) 1.25 µg of labeled junction 6 wt-p2 ssDNA, (3) 2.2 µg of 28-nt DNA splint, (4) 28-nt DNA-splinted ligation of junction 6 wt-p1 ssDNA to junction 6 wt-p2 ssDNA, side-products were not observed after ligation, (5) 1.5 µg of purified 39-nt junction 6 wt ssDNA. Bands are visualized with Stains-All (Acros Organics, Geel, Belgium).

6 wt, respectively. After digestion of the 50 bp three-way junction dsDNA fragments with *Eco*RI and 35 bp junction 6 wt-p2 dsDNA fragments with *Xho*I, distinguishable bands were observed on a 20% denaturing PAGE (Figure 4A and B, lanes 2 and 1, respectively). From these bands, excised from a preparative denaturing gel, DNA was purified yielding 675 µg (0.06 µmol) three-way junction ssDNA and 450 µg (0.073 µmol) 20-nt junction 6 wt-p2 ssDNA. Circa 43% (54% for the three-way junction and 32% of junction 6 wt) of the 7.2 µmol of input labeled dCTPs were incorporated into the final PCR product (50 and 35 bp products, see above). Overall ~10% of the labeled dCTPs become incorporated in the purified target ssDNAs (~10% for the three-way junction and ~9% for junction 6 wt).

Ligation of the labeled 20-nt junction 6 wt-p2 to the unlabeled 19-nt junction 6 wt-p1 assisted by the 28-nt DNA splint into 39-nt junction 6 wt ssDNA, resulted in a yield of ~95% (visual estimation from gel; Figure 4C, lane 4; UV of final pure product showed that the actual yield was 85%). After purification, 750 µg (0.062 µmol) of segmental selective labeled junction 6 wt ssDNA was obtained.

NMR experiments

Thanks to the stereo-selective deuteration of the H2″ in the three-way junction ssDNA, the stereo-specific resonance assignment of H2′ can easily be obtained via H2′(C2′)C1′ correlation (Figure 5A) in combination with H2′C2′ correlation (Figure 5B). The labeling of dT residues in segment C20–C39 of junction 6 wt ssDNA is illustrated in Figures 5C and D. Comparison of the 1D traces in Figure 5C shows that only labeled dT imino resonances (of A:T base pairs) remain upon ^{15}N-filtering. In the 2D HSQC (Figure 5D) only two dT imino cross-peaks are expected, given the secondary structure and the segmental labeling (Figure 2C). We observe one strong cross peak, which can be attributed to T35 in the lower stem. However, instead of the expected single cross-peak for T32, two (weaker) cross-peaks are seen, indicating multiple conformations at the junction.

DISCUSSION

We have shown that self-primed PCR of DNA combined with asymmetrical double digestion of the PCR product and *in vitro* dNTP synthesis forms an efficient and straightforward method for obtaining NMR amounts of (stereo-)selective and/or segmental ^{2}H/^{13}C/^{15}N-labeled ssDNA. A host of labeling patterns is possible, thereby making NMR structural studies on (larger) ssDNA more accessible. With this labeling, NMR spectral crowding is reduced, specific resonances can be eliminated or selected and line widths reduced by deuteration.

Synthesis of selective and/or segmentally labeled ssDNA and dNTPs

The amplification of the DNA primers by means of self-primed PCR followed by double digestion requires attention to their design. The sequences should not become trapped in duplexes or intramolecular structures blocking PCR. When DINAMelt predicts such alternative stable structures, the spacer fragment can be shortened, lengthened or altered. The role of the spacer is essentially only to facilitate efficient restriction endonuclease digestion in the second digestion step and is of no further interest.

Furthermore, potentially any restriction site can be chosen to flank the DNA fragment of interest. Amongst the wide variety of available enzymes, it is likely that a combination can be found that generates digested ends exactly matching the 5′-end- and 3′-end of the DNA fragment of interest. Our method is based on the difference in migration distance on denaturing PAGE of the asymmetric DNA fragments that are generated thanks to the sticky-end restriction endonuclease digestion. In both described cases, the asymmetry comprises 5′-recessing ends of 4-nt. For ssDNAs up to 50-nt, this 4-nt overhang is sufficient for separation on preparative denaturing polyacrylamide gels. Larger ssDNAs can be obtained by applying the first endonuclease digestion with a

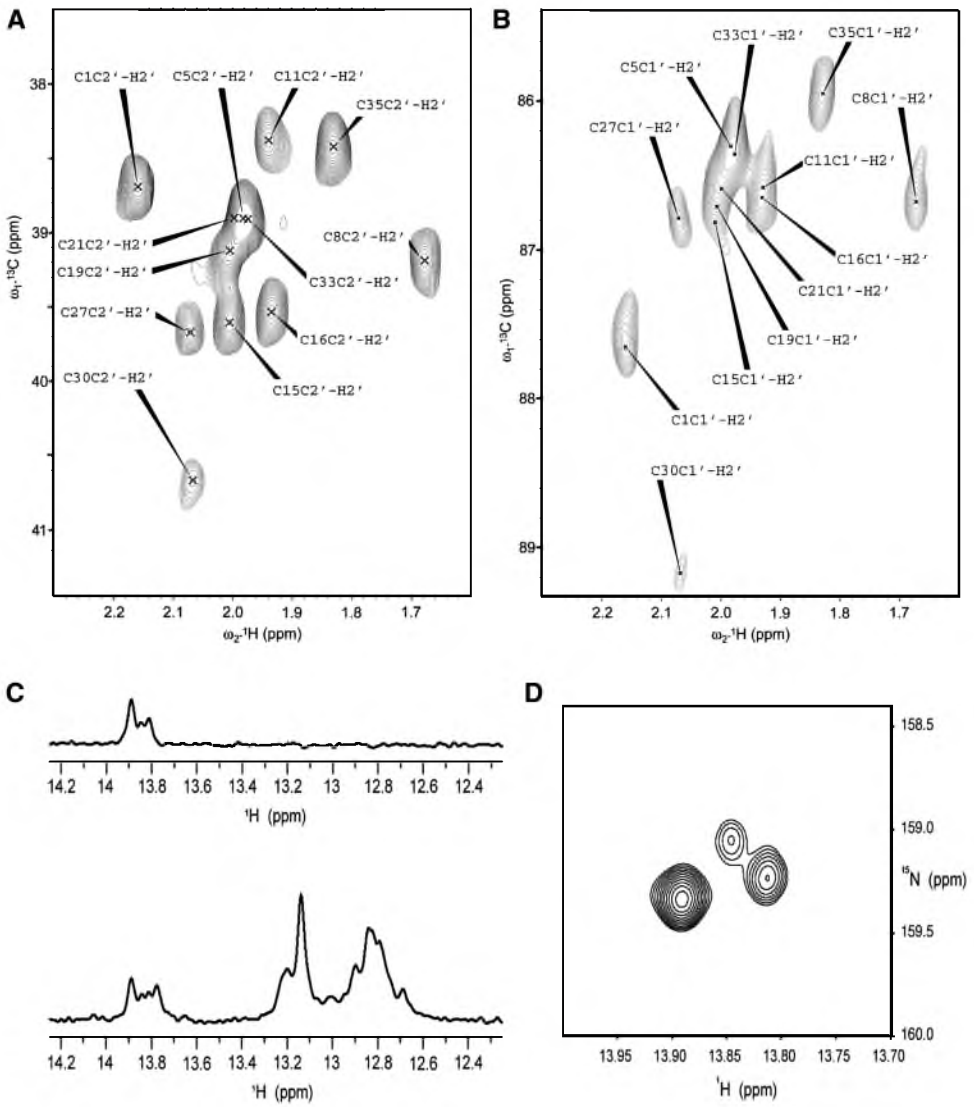

Figure 5. NMR spectra of the prepared labeled ssDNAs. (**A**) (C2′, H2′) and (**B**) (C1′, H2′) region of a 2D H2′C2′C1′ spectrum of the selective $^{13}C_9/^{15}N_3/^{2}H_{(1',2'',3',4',5',5'')}$-dC-labeled three-way junction; the spectrum is used for stereo-specific assignment of the H2′ resonances in the ribose of the labeled dC residues. (**C**) 1D proton spectra of the imino protons of segmental (C20–C39) $^{13}C_9/^{15}N_2/^{2}H_{(1',2'',3',4',5',5'')}$-dT and $^{13}C_9/^{15}N_3/^{2}H_{(1',2'',3',4',5',5'')}$-dC-labeled junction 6 wt with (top) and without (bottom) filter for ^{15}N-editing. (**D**) Imino region of a 2D (^{15}N, ^{1}H) HSQC displaying the signals of ^{15}N-labeled thymidines of the segmental labeled junction 6 wt.

3′-recessing-end generating endonuclease. With the resulting 8-nt difference, ssDNA molecules up to 75-nt can be separated.

Finally, 54% and 32% of the labeled dCTPs are incorporated into the final PCR product for the three-way junction and junction 6 wt-p2. These yields are comparable to the ~50% of Louis *et al.* (45). Most of the minor loss could be due to instability of dNTPs over the extended heating/cooling cycles (60–95°C) in the PCR. For instance, deamination of dCTP leading to dUTP may occur, as well as aspecific dephosphorylation to dCMP (67). Finally, the *in vitro* synthesis of dCTP and dTTP is not limiting as they are produced with ~80% yields from their rNTP counterparts. In our experience these yields are attained when applying standard optimization parameters for PCR, such as annealing temperature, Mg^{2+}-concentration, etc. To improve yields (e.g. the 32%) most effective would be to increase the number of PCR cycles. In the final ssDNAs for both the three-way junction and junction 6 wt-p2 ~10% of the labeled dCTP is incorporated. Part of the loss in the last step (compare with 54% and 32%) is due to the fact that the target ssDNAs contains only 38% and 45% of the cytidines present in the complete PCR repeat (see e.g. Table 1); further losses are due to a combination of incomplete digestion and purification steps.

A high yield (~95%) was obtained in the splinted ligation by T4 DNA ligase of the two DNA segments into the junction 6 wt ssDNA. We previously observed that (DNA-)splinted ligation of RNA segments using T4 DNA ligase is in general quite robust and leads to high yields (27). Nevertheless, it is crucial for successful (DNA-)splinted ligation of two ssDNA segments to verify optimal formation of the desired hybridization product.

This information can be obtained from DINAMelt simulations. Finally, our segmental labeling method can be extended to more than two segments without significant loss in ligation yield, e.g. by designing two nicks on a hybrid of three segments with a DNA splint or by using two DNA splints and three segments in one ligation reaction.

CONCLUSION

We propose and show that self-primed PCR of DNA combined with asymmetrical double digestion of the PCR product and *in vitro* dNTP synthesis forms an efficient and straightforward method for obtaining NMR amounts of (stereo-)selective and/or segmental $^{2}H/^{13}C/^{15}N$-labeled ssDNA.

SUPPLEMENTARY DATA

Supplementary Data are available at NAR Online.

ACKNOWLEDGEMENTS

Funding within the context of the 6th framework program of the EU, 6th framework STREP project FSG-V-RNA is gratefully acknowledged.

FUNDING

Funding for open access charge: Department of Biophysical Chemistry of the Radboud University Nijmegen, The Netherlands.

REFERENCES

1. Sattler,M., Schleucher,J. and Griesinger,C. (1999) Heteronuclear multidimensional NMR experiments for the structure determination of proteins in solution employing pulsed field gradients. *Prog. NMR Spec.*, **34**, 93–158.
2. Tugarinov,V., Hwang,P.M. and Kay,L.E. (2004) Nuclear magnetic resonance spectroscopy of high-molecular-weight proteins. *Annu. Rev. Biochem.*, **73**, 107–146.
3. Kontaxis,G., Delaglio,F. and Bax,A. (2005) Molecular fragment replacement approach to protein structure determination by chemical shift and dipolar homology database mining. *Methods Enzymol.*, **394**, 42–49.
4. Prestegard,J.H., Mayer,K.L., Valafar,H. and Benison,G.C. (2005) Determination of protein backbone structures from residual dipolar couplings. *Methods Enzymol.*, **394**, 175–185.
5. Korzhnev,D.M. and Kay,L.E. (2008) Probing invisible, low-populated states of protein molecules by relaxation dispersion NMR spectroscopy: An application to protein folding. *Acc. Chem. Res.*, **41**, 442–451.
6. Batey,R.T., Inada,M., Kujawinski,E., Puglisi,J.D. and Williamson,J.R. (1992) Preparation of isotopically labeled ribonucleotides for multidimensional NMR-spectroscopy of RNA. *Nucleic Acids Res.*, **20**, 4515–4523.
7. Nikonowicz,E.P., Sirr,A., Legault,P., Jucker,F.M., Baer,L.M. and Pardi,A. (1992) Preparation of ^{13}C and ^{15}N labelled RNAs for heteronuclear multi-dimensional NMR studies. *Nucleic Acids Res.*, **20**, 4507–4513.
8. Foldesi,A., Yamakage,S.I., Nilsson,F.P., Maltseva,T.V. and Chattopadhyaya,J. (1996) The use of non-uniform deuterium labelling ['NMR-window'] to study the NMR structure of a 21mer RNA hairpin. *Nucleic Acids Res.*, **24**, 1187–1194.
9. Tolbert,T.J. and Williamson,J.R. (1997) Preparation of specifically deuterated and ^{13}C-labeled RNA for NMR studies using enzymatic synthesis. *J. Am. Chem. Soc.*, **119**, 12100–12108.
10. Wijmenga,S.S., Heus,H.A., Leeuw,H.A.E., Hoppe,H., Vandergraaf,M. and Hilbers,C.W. (1995) Sequential backbone assignment of uniformly ^{13}C-labeled RNAs by a 2-dimensional P(CC)H-TOCSY triple-resonance NMR experiment. *J. Biomol. NMR*, **5**, 82–86.
11. Wijmenga,S.S. and van Buuren,B.N.M. (1998) The use of NMR methods for conformational studies of nucleic acids. *Prog. NMR Spec.*, **32**, 287–387.
12. Cromsigt,J.A.M.T.C., Schleucher,J., Kidd-Ljunggren,K. and Wijmenga,S.S. (2000) Synthesis of specifically deuterated nucleotides for NMR studies on RNA. *J. Biomol. Struct. Dyn.*. 211–219.
13. Cromsigt,J., van Buuren,B., Schleucher,J. and Wijmenga,S. (2001) Resonance assignment and structure determination for RNA. *Methods Enzymol.*, **338**, 371–399.
14. Nikonowicz,E.P. (2001) Preparation and use of ^{2}H-labeled RNA oligonucleotides in nuclear magnetic resonance studies. *Methods Enzymol.*, **338**, 320–341.
15. Cromsigt,J., Schleucher,J., Gustafsson,T., Kihlberg,J. and Wijmenga,S. (2002) Preparation of partially $^{2}H/^{13}C$-labelled RNA for NMR studies. Stereo-specific deuteration of the H5″ in nucleotides. *Nucleic Acids Res.*, **30**, 1639–1645.
16. Kim,I., Lukavsky,P.J. and Puglisi,J.D. (2002) NMR study of 100 kDa HCV IRES RNA using segmental isotope labeling. *J. Am. Chem. Soc.*, **124**, 9338–9339.
17. Flodell,S., Schleucher,J., Cromsigt,J., Ippel,H., Kidd-Ljunggren,K. and Wijmenga,S. (2002) The apical stem-loop of the hepatitis B virus encapsidation signal folds into a stable tri-loop with two underlying pyrimidine bulges. *Nucleic Acids Res.*, **30**, 4803–4811.
18. Furtig,B., Richter,C., Wohnert,J. and Schwalbe,H. (2003) NMR spectroscopy of RNA. *Chembiochem*, **4**, 936–962.
19. Latham,M.R., Brown,D.J., McCallum,S.A. and Pardi,A. (2005) NMR methods for studying the structure and dynamics of RNA. *Chembiochem*, **6**, 1492–1505.
20. Al-Hashimi,H.M. (2005) Dynamics-based amplification of RNA function and its characterization by using NMR spectroscopy. *Chembiochem*, **6**, 1506–1519.
21. Flinders,J. and Dieckmann,T. (2006) NMR spectroscopy of ribonucleic acids. *Prog. NMR Spec.*, **48**, 137–159.
22. Tzakos,A.G., Grace,C.R.R., Lukavsky,P.J. and Riek,R. (2006) NMR techniques for very large proteins and RNAs in solution. *Annu. Rev. Biophys. Biomol. Struct.*, **35**, 319–342.
23. Getz,M., Sun,X.Y., Casiano-Negroni,A., Zhang,Q. and Al-Hashimi,H.M. (2007) NMR studies of RNA dynamics and structural plasticity using NMR residual dipolar couplings. *Biopolymers*, **86**, 384–402.
24. Bailor,M.H., Musselman,C., Hansen,A.L., Gulati,K., Patel,D.J. and Al-Hashimi,H.M. (2007) Characterizing the relative orientation and dynamics of RNA A-form helices using NMR residual dipolar couplings. *Nature Protocols*, **2**, 1536–1546.
25. Ponchon,L. and Dardel,F. (2007) Recombinant RNA technology: the tRNA scaffold. *Nature Methods*, **4**, 571–576.
26. Dayie,K.T. (2008) Key labeling technologies to tackle sizeable problems in RNA structural biology. *Int. J. Mol. Sci.*, **9**, 1214–1240.
27. Nelissen,F.H.T., van Gammeren,A.J., Tessari,M., Girard,F.C., Heus,H.A. and Wijmenga,S.S. (2008) Multiple segmental and selective isotope labeling of large RNA for NMR structural studies. *Nucleic Acids Res.*, **36**, e89.
28. Shajani,Z. and Varani,G. (2007) NMR studies of dynamics in RNA and DNA by ^{13}C relaxation. *Biopolymers*, **86**, 348–359.
29. Kojima,C., Ono,A., Kainosho,M. and James,T.L. (1998) DNA duplex dynamics: NMR relaxation studies of a decamer with uniformly ^{13}C-labeled purine nucleotides. *J. Magn. Reson.*, **135**, 310–333.
30. Foldesi,A., Maltseva,T.V. and Chattopadhyaya,J. (1999) The application of "the Uppsala NMR-window" concept for conformational analysis of large DNA & RNA by high-field NMR spectroscopy. *Nucleosides and Nucleotides*, **18**, 1599–1600.
31. Maltseva,T.V., Foldesi,A. and Chattopadhyaya,J. (1999) Measurement of the deuterium relaxation times in double-labeled ($^{13}C/^{2}H$) thymidine and 2′-deoxyadenosine and in the selectively

labeled DNA duplex $^{5'}d(^{1}C^{2}G^{3}\underline{A}^{4}\underline{T}^{5}\underline{T}^{6}\underline{A}^{7}\underline{A}^{8}\underline{T}^{9}C^{10}G)_2{}^{3'}$. *Magn. Reson. Chem.*, **37**, 203–213.
32. Kojima,C., Ono,A. and Kainosho,M. (2000) Studies of physicochemical properties of N-H···N hydrogen bonds in DNA, using selective ^{15}N-labeling and direct ^{15}N 1D NMR. *J. Biomol. NMR*, **18**, 269–277.
33. van Buuren,B.N.M., Overmars,F.J.J., Ippel,J.H., Altona,C. and Wijmenga,S.S. (2000) Solution structure of a DNA three-way junction containing two unpaired thymidine bases. Identification of sequence features that decide conformer selection. *J. Mol. Biol.*, **304**, 371–383.
34. Kojima,C., Ono,A.M., Ono,A. and Kainosho,M. (2001) Solid-phase synthesis of selectively labeled DNA: Applications for multidimensional nuclear magnetic resonance spectroscopy. *Methods Enzymol.*, **338**, 261–283.
35. van Buuren,B.N.M., Hermann,T., Wijmenga,S.S. and Westhof,E. (2002) Brownian-dynamics simulations of metal-ion binding to four-way junctions. *Nucleic Acids Res.*, **30**, 507–514.
36. Wu,Z.G., Delaglio,F., Tjandra,N., Zhurkin,V.B. and Bax,A. (2003) Overall structure and sugar dynamics of a DNA dodecamer from homo and heteronuclear dipolar couplings and ^{31}P chemical shift anisotropy. *J. Biomol. NMR*, **26**, 297–315.
37. van Buuren,B.N.M., Schleucher,J., Wittmann,V., Griesinger,C., Schwalbe,H. and Wijmenga,S.S. (2004) NMR spectroscopic determination of the solution structure of a branched nucleic acid from residual dipolar couplings by using isotopically labeled nucleotides. *Angew. Chem. Int. Edit.*, **43**, 187–192.
38. Fernandez,C., Szyperski,T., Ono,A., Iwai,H., Tate,S., Kainosho,M. and Wuthrich,K. (1998) NMR with ^{13}C, ^{15}N-doubly-labeled DNA: The Antennapedia homeodomain complex with a 14-mer DNA duplex. *J. Biomol. NMR*, **12**, 25–37.
39. Allen,M., Varani,L. and Varani,G. (2001) Nuclear magnetic resonance methods to study structure and dynamics of RNA–protein complexes. *Methods Enzymol.*, **339**, 357–376.
40. Wu,H.H., Finger,L.D. and Feigon,J. (2005) Structure determination of protein/RNA complexes by NMR. *Methods Enzymol.*, **394**, 525–545.
41. Mackereth,C.D., Simon,B. and Sattler,M. (2005) Extending the size of protein-RNA complexes studied by nuclear magnetic resonance spectroscopy. *Chembiochem*, **6**, 1578–1582.
42. Williamson,J.R. and Boxer,S.G. (1988) Synthesis of a thymidine phosphoramidite labeled with ^{13}C at C6 – relaxation studies of the loop region in a ^{13}C-labeled DNA hairpin. *Nucleic Acids Res.*, **16**, 1529–1540.
43. Kellenbach,E.R., Remerowski,M.L., Eib,D., Boelens,R., Vandermarel,G.A., Vandenelst,H., Vanboom,J.H. and Kaptein,R. (1992) Synthesis of isotope labeled oligonucleotides and their use in an NMR-study of a protein–DNA complex. *Nucleic Acids Res.*, **20**, 653–657.
44. Ono,A., Tate,S., Ishido,Y. and Kainosho,M. (1994) Preparation and heteronuclear 2D NMR-spectroscopy of a DNA dodecamer containing a thymidine residue with a uniformly ^{13}C-labeled deoxyribose ring. *J. Biomol. NMR*, **4**, 581–586.
45. Louis,J.M., Martin,R.G., Clore,G.M. and Gronenborn,A.M. (1998) Preparation of uniformly isotope-labeled DNA oligonucleotides for NMR spectroscopy. *J. Biol. Chem.*, **273**, 2374–2378.
46. Ramanathan,S., Rao,B.J. and Chary,K.V.R. (2002) A novel approach for uniform ^{13}C and ^{15}N labeling of DNA for NMR studies. *Biochem. Biophys. Res. Comm.*, **290**, 928–932.
47. Zimmer,D.P. and Crothers,D.M. (1995) NMR of enzymatically synthesized uniformly ^{13}C^{15}N-labeled DNA oligonucleotides. *Proc. Natl Acad. Sci. USA*, **92**, 3091–3095.
48. Smith,D.E., Su,J.Y. and Jucker,F.M. (1997) Efficient enzymatic synthesis of ^{13}C,^{15}N-labeled DNA for NMR studies. *J. Biomol. NMR*, **10**, 245–253.
49. Masse,J.E., Bortmann,P., Dieckmann,T. and Feigon,J. (1998) Simple, efficient protocol for enzymatic synthesis of uniformly ^{13}C,^{15}N-labeled DNA for heteronuclear NMR studies. *Nucleic Acids Res.*, **26**, 2618–2624.
50. Mer,G. and Chazin,W.J. (1998) Enzymatic synthesis of region-specific isotope-labeled DNA oligomers for NMR analysis. *J. Am. Chem. Soc.*, **120**, 607–608.
51. Rudert,W.A. and Trucco,M. (1990) DNA polymers of protein-binding sequences generated by PCR. *Nucleic Acids Res.*, **18**, 6460–6460.
52. White,M.J., Fristensky,B.W. and Thompson,W.F. (1991) Concatemer chain-reaction—a *Taq* DNA Polymerase-mediated mechanism for generating long tandemly repetitive DNA-sequences. *Anal. Biochem.*, **199**, 184–190.
53. Chen,X., Mariappan,S.V.S., Kelley,J.J., Bushweller,J.H., Bradbury,E.M. and Gupta,G. (1998) A PCR-based method for uniform ^{13}C/^{15}N labeling of long DNA oligomers. *FEBS Lett.*, **436**, 372–376.
54. Yan,J.L. and Bushweller,J.H. (2001) An optimized PCR-based procedure for production of ^{13}C/^{15}N-labeled DNA. *Biochem. Biophys. Res. Comm.*, **284**, 295–300.
55. Werner,M.H., Gupta,V., Lambert,L.J. and Nagata,T. (2001) Uniform ^{13}C/^{15}N-labeling of DNA by tandem repeat amplification. *Methods Enzymol.*, **338**, 283–304.
56. Rene,B., Masliah,G., Zargarian,L., Mauffret,O. and Fermandjian,S. (2006) General method of preparation of uniformly ^{13}C, ^{15}N-labeled DNA fragments for NMR analysis of DNA structures. *J. Biomol. NMR*, **36**, 137–146.
57. Muecke,M., Samuels,M., Davey,M. and Jeruzalmi,D. (2008) Preparation of multimilligram quantities of large, linear DNA molecules for structural studies. *Structure*, **16**, 837–841.
58. Hoard,D.E. and Ott,D.G. (1965) Conversion of mono- and oligodeoxyribonucleotides to 5′-triphosphates. *J. Am. Chem. Soc.*, **87**, 1785–1788.
59. Wu,B., Girard,F., van Buuren,B., Schleucher,J., Tessari,M. and Wijmenga,S. (2004) Global structure of a DNA three-way junction by solution NMR: towards prediction of 3H fold. *Nucleic Acids Res.*, **32**, 3228–3239.
60. Panigrahi,G.B., Lau,R., Montgomery,S.E., Leonard,M.R. and Pearson,C.E. (2005) Slipped (CTG)·(CAG) repeats can be correctly repaired, escape repair or undergo error-prone repair. *Nat. Struct. Mol. Biol.*, **12**, 654–662.
61. Panigrahi,G.B., Cleary,J.D. and Pearson,C.E. (2002) *In vitro* (CTG)·(CAG) expansions and deletions by human cell extracts. *J. Biol. Chem.*, **277**, 13926–13934.
62. Markham,N.R. and Zuker,M. (2005) DINAMelt web server for nucleic acid melting prediction. *Nucleic Acids Res.*, **33**. W577–W581.
63. Tolbert,T.J. and Williamson,J.R. (1996) Preparation of specifically deuterated RNA for NMR studies using a combination of chemical and enzymatic synthesis. *J. Am. Chem. Soc.*, **118**, 7929–7940.
64. Bearne,S.L., Hekmat,O. and MacDonnell,J.E. (2001) Inhibition of *Escherichia coli* CTP synthase by glutamate gamma-semialdehyde and the role of the allosteric effector GTP in glutamine hydrolysis. *Biochem. J.*, **356**, 223–232.
65. Booker,S. and Stubbe,J. (1993) Cloning, sequencing, and expression of the adenosylcobalamin-dependent ribonucleotide reductase from *Lactobacillus leichmannii*. *Proc. Natl Acad. Sci. USA*, **90**. 8352–8356.
66. MacDonald,D. and Lu,P.Z. (2002) Determination of DNA structure in solution: enzymatic deuteration of the ribose 2′ carbon. *J. Am. Chem. Soc.*, **124**, 9722–9723.
67. Dabrowski,S. and Ahring,B.K. (2003) Cloning, expression, and purification of the His_6-tagged hyper-thermostable dUTPase from *Pyrococcus woesei* in *Escherichia coli*: application in PCR. *Protein Expr. Purif.*, **31**, 72–78.
68. Changchien,L.M., Garibian,A., Frasca,V., Lobo,A., Maley,G.F. and Maley,F. (2000) High-level expression of *Escherichia coli* and *Bacillus subtilis* thymidylate synthases. *Protein Expr. Purif.*, **19**. 265–270.
69. Mikoulinskaia,G.V., Zimin,A.A., Feofanov,S.A. and Miroshnikov,A.I. (2004) Identification, cloning, and expression of bacteriophage T5 *dnk* gene encoding a broad specificity deoxyribonucleoside monophosphate kinase (EC 2.7.4.13). *Protein Expr. Purif.*, **33**, 166–175.
70. Dabrowski,S. and Kur,J. (1998) Cloning and expression in *Escherichia coli* of the recombinant His-tagged DNA polymerases from *Pyrococcus furiosus* and *Pyrococcus woesei*. *Protein Expr. Purif.*, **14**, 131–138.